A R C H I V E S O F M E T A L L U R G Y A N D M A T E R I A L S
Volume 60 2015 Issue 4
DOI: 10.1515/amm-2015-0407

A. DĘBSKI*, M. H. BRAGA**, W. GĄSIOR*,#

THE B-Li SYSTEM. CALORIMETRIC AND THEORETICAL STUDIES

UKŁAD B-Li. BADANIA KALORYMETRYCZNE I TEORETYCZNE

The standard enthalpy of formation of the $B_{78}Li_{22}$ alloy was measured with the use of the water reaction calorimetric method at 25 °C (298 K). An X-ray diffraction study of the prepared sample was conducted. The obtained diffraction pattern was different from the patterns for the B_3Li and $B_{14}Li_3$ phases. The standard enthalpy of formation obtained for the $B_{78}Li_{22}$ alloy was -39.0 ± 0.7 kJ/mole of atoms. This value corresponds well with the formation enthalpies of the phases from the boron-lithium system. Theoretical calculations of the standard enthalpy of formation were conducted for the $B_{78}Li_{22}$ alloy and the phases from B-Li system, which were investigated earlier. A discussion of the deviations observed between both sets of data (experimental and calculated) was performed. Additionally, DTA studies were performed for 14 alloys of the concentrations from 40 to 100 at. % of Li.

Keywords: Phase diagrams, Thermodynamic and thermochemical properties, Ab-initio calculations, Calorimetry.

Standardowa entalpia tworzenia stopu $B_{78}Li_{22}$ została zmierzona metodą kalorymetrii reakcyjnej wodnej. Próbka stopu po wyżarzaniu była poddana badaniom strukturalnym metodą dyfrakcji promieniowania rentgenowskiego. Uzyskany dyfraktogram jest inny od dyfraktogramów dla faz B_3Li ora $B_{14}Li_3$. Zmierzona standardowa entalpia tworzenia stopu $B_{78}Li_{22}$ wyniosła -39.0 ± 0.7 kJ/mol atomów. Wartość ta dobrze koreluje z entalpią tworzenia faz z układu bor-lit. Przeprowadzone zostały również obliczenia teoretyczne standardowej entalpii tworzenia dla stopu $B_{78}Li_{22}$ oraz faz z układu B-Li, wcześniej badanych. Zaobserwowane rozbieżności między teoretycznymi i eksperymentalnymi wartościami entalpii tworzenia zostały przedyskutowane. Ponadto, wykonano pomiary DTA dla 14 stopów o stężeniach od 40 do 100 % at. Li.

1. Introduction

The great interest in the application of hydrogen as fuel has been caused by the exhaustion of the traditional fuel sources and by the world ecological tendency to decrease the carbon dioxide emission. Hydrogen can be regarded as a completely ecological fuel because water is its combustion product. However, the use of hydrogen as fuel is drastically reduced because of the difficulty of its transportation and storage. Therefore, the search for safe storage methods and the use of hydrogen fuel is a vital objective for many laboratories all over the world. One of the storage solutions proposed is in the form of metal hydrides. Although the compound $LiBH_4$ can theoretically store up to 19 wt. % of hydrogen, the interest in measuring the thermodynamic properties of the B-Li system seems to be rather weak. Boron-lithium alloys of a high Li concentration can also be used as anode materials in high temperature lithium batteries because of the low density and the lithium-comparable electrochemical properties.

In 1932, Andrieux and Barbetti [1] initiated the investigations of the B-Li system and obtained the B_6Li phase using the electrochemical technique. In 1974, Rupp and Hodges [2] studied the conduction-electron spin resonance in the compound B_6Li. Other phases of the B-Li system were proposed by [3, 4] – $B_{12}Li$, [5, 6] – B_4Li, [7] – B_3Li, [3, 4, 8, 9] – B_2Li, [10] – BLi, [6, 7, 9] - B_4Li_5 (B_6Li_7), [7, 11] - BLi_3 and [12] - $B_{14}Li_3$, $B_{19}Li_6$, first based on electromotive force, density and electrical resistivity measurements. During the subsequent years, some of them were confirmed by XRD studies [12-15]. Additionally, Mair et al. [12] prepared and investigated a single crystal of B_3Li and found that, in fact, the B_3Li compound is composed of 6 atoms of boron and 2 atoms of lithium (B_6Li_2), that its structure is tetragonal (tP16) and that it belongs to the P4/mbm space group.

The number of papers on the thermodynamics of the B-Li system is very limited, which is probably caused by the need for a very pure atmosphere of a noble protective gas, both for the preparation and the performing of the experiments. It was possible to find two studies [6, 8] on the discharge behavior of B-Li alloys between 400-600°C (673-873 K), and articles [6, 16-22] reporting heat effects on B-Li during the thermal analysis. The information on the preparation and investigations

* INSTITUTE OF METALLURGY AND MATERIALS SCIENCE, POLISH ACADEMY OF SCIENCES, 30-059 KRAKÓW, REYMONTA STREET 25, POLAND
** CEMUC, PHYSICS ENGINEERING DEPARTMENT, ENGINEERING FACULTY OF THE UNIVERSITY OF PORTO, R. DR. ROBERTO FRIAS S/N, 4200-465 PORTO, PORTUGAL.
# Corresponding author: gasior@imim.pl

of the B-Li alloys or phases as well as the theoretical studies of their various properties was found in studies [23,24].

In 1989, Okamoto [25] collected information on the investigations of the B-Li system and presented all the phases which were suggested in the literature ($B_{13}Li$, B_6Li, $B_{14}Li_3$, B_4Li, B_3Li, B_2Li, BLi, BLi_3), and in 2003, Borgstedt and Gumiński [26] proposed the part of the B-Li phase diagram which also took into consideration the liquidus and solidus temperatures presented in [27] for alloys of the Li concentration between 0.5 and 1 mole fraction, beside the B_4Li, BLi_3 and B_2Li phases.

In a publication from 2013 [28], Aydin studied the structural, mechanical and electronic properties of B_6Li_2 and Herman et al. [29], studied the Li-B system using the first principles calculations to determine the influence of pressure on the stability of the compounds. Also, a few new compounds stabilizing with pressure (up to 320 GPa) were found. Herman et al. [29] came to very similar conclusions at 0 K and 1 atm. as we did and are going to present herein; nonetheless, they did not study the temperature dependence on the stability of the compounds. Moreover, the latter authors did not study the phases $B_{13}Li$ and B_7Li, which were experimentally obtained, claiming that these phases exhibit huge unit cells. In spite of this, we decided to present the first principles results for them, and in the later part of this paper, we will discuss the calculation results.

This paper is a continuation of our study on the heat of formation of the intermediate phases of the B-Li system [30-31]. The X-ray diffraction (XRD) pattern of the $B_{78}Li_{22}$ alloy together with the XRD pattern of the B_3Li and $B_{14}Li_3$ phases will be analyzed as well as the experimental data of the standard enthalpy of formation of $B_{78}Li_{22}$ obtained by the calorimetric reaction technique. Additionally, Differential Thermal Analysis (DTA) experiments were performed. First principles (DFT) as well as phonon calculations were additionally performed for a thermal stability analysis and a comparison with the experimental results.

The Density Functional Theory (DFT) results for $B_{10\text{-}13}Li$ and $B_{6\text{-}7}Li$, and $B_{155}Li_{12}$ and $B_{112}Li_{13}$, respectively, as well as the phonon results will allow us to understand the stability dependence on the temperature for these phases, which, to the best of our knowledge, were herein optimized for the first time.

2. Experimental

2.1. Calorimetric study

The enthalpy of formation measurements of the $B_{78}Li_{22}$ alloy were performed by the calorimetric reaction technique, which was described in detail in our previous work [30].

2.2. Differential Thermal Analysis (DTA)

Phase transformation as well as liquidus and solidus temperature measurements of the B-Li alloys were conducted by the DTA technique with the use of a Q-1500 (Paulik-Paulik-Erdey) derivatograph. The samples were prepared in the MBraun glove-box filled with high purity argon, similarly to our previous calorimetric measurements [30-31]. The alloys were prepared by way of melting the metals in Mo crucibles with a cover, which were placed in Ni crucibles and sealed with a Ni stopper by means of a hydraulic press. The weights of the test samples were ~0.2 g. Afterwards, the DTA measurements were performed in air with the temperature rate of 5 K/min, with the use of empty Ni and Mo crucibles as reference.

2.3. Preparation and identification of $B_{78}Li_{22}$ alloy

The $B_{78}Li_{22}$ alloy used in the water reaction calorimetric experiments was prepared by a synthesis of boron (pieces of purity 99.5 wt. %) with lithium (rod of purity 99.9 wt. %) delivered by Alfa-Aesar. The stoichiometric amounts of B and Li were slowly heated in the Mo crucible in the glove box up to 1000ºC (1273 K), annealed for 4 hours, and subsequently cooled together with the furnace to room temperature. The prepared sample of the alloy was analyzed by means of XRD (Philips PW 1710 Diffractometer with Co-Kα filtered radiation), for the confirmation of its structure. For the identification of the phases, the EVA (Bruker) computer program was used. The XRD pattern of the $B_{78}Li_{22}$ alloy is shown in Figure 1.

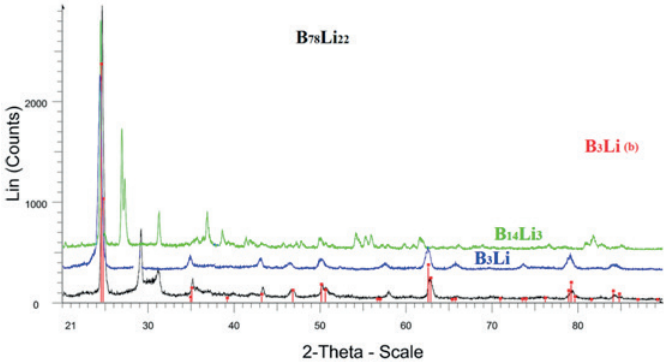

Fig. 1. X-ray diffraction pattern of $B_{78}Li_{22}$ (black line), B_3Li (blue line) and $B_{14}Li_3$ (green line)

As presented in Fig. 1, the X-ray diffraction pattern of $B_{78}Li_{22}$ is different from that of $B_{14}Li_3$ and B_3Li, which may suggest the existence of an intermetallic compound with the composition of $0.176 < X(Li) < 0.220$. Taking into account the study of L.E. DeVries et al. [6], the observed diffraction pattern in Fig. 1 may be that of the B_4Li phase.

3. Calculations

One of the most important methods of quantum mechanical modelling of solids is the framework of the Density Functional Theory (DFT) [33], which uses the Generalized Gradient Approximation (GGA) [34].

DFT calculations with Projector Augmented Wave (PAW) pseudopotentials [35], and the Perdew–Burke–Ernzerhof (PBE) functional [36] were used as implemented in the Vienna Ab Initio Simulation Package (VASP) code [37]. A plane wave cut off at least 400.00 eV and k-spacing of 0.230 × 0.230 × 0.230 $Å^{-1}$ were used. The calculations were performed in the real space, for: B (beta_rhombo-B), $B_{155}Li_{12}$, $B_{13}Li$, $B_{112}Li_{13}$,

B_7Li, $B_{87}Li_{13}$ $B_{14}Li_3$, B_4Li, $B_{42}Li_{11}$, $B_{24}Li_7$, $B_{16}Li_5$, $B_{72}Li_{23}$, B_3Li, $B_{47}Li_{16}$, BLi, B_5Li_6, B_4Li_5, and Li (bcc-A2). Each phase was calculated for different space groups; we tried to optimize each phase with a structure and stoichiometry as similar as possible to the corresponding published versions. The total energy was minimized with respect to the volume (volume relaxation), the shape of the unit cell (external relaxation), and the position of the atoms within the cell (internal relaxation). For more details on the crystal structures of the stable phases, please check the Supplement.

The phonon direct method [38] was applied to predict the lattice dynamics with the use of the harmonic approximation in VASP's minimized structures which had the lowest ground state energy. Therefore, the electronic structure at the ground state was calculated with the use of VASP and the zero point energy, while the phonons' energy and the entropy were calculated with the use of Phonon. In fact, we calculated the Helmholtz free energy, which can be approximated to the Gibbs free energy at zero stress.

With the use of the vibration frequencies ω, the Helmholtz free energy, the internal energy - which can be approximated to the enthalpy - and the entropy were calculated as follows:

$$F_{phonon} = 3Nk_BT\int_0^{\omega_L} ln\left(2sinh\frac{\hbar\omega}{2k_BT}\right)g(\omega)d\omega \quad (1)$$

$$E_{phonon} = 3N\frac{\hbar}{2}\int_0^{\omega_L} \omega coth\left(\frac{\hbar\omega}{2k_BT}\right)g(\omega)d\omega \quad (2)$$

$$S_{phonon} = 3Nk_B\int_0^{\omega_L}\left[\frac{\hbar\omega}{2k_BT}coth\left(\frac{\hbar\omega}{2k_BT}\right) - ln\left(2sinh\frac{\hbar\omega}{2k_BT}\right)\right]g(\omega)d\omega \quad (3)$$

where: N is the number of atoms in the cell, k_B is Boltzmann's constant, T is the absolute temperature, ω_L is the maximal frequency and g(ω) is the frequency distribution function. Therefore, adding the electronic contribution, *Eelec*, calculated with the use of DFT, as implemented in VASP, the *ZPE* zero-point energy of the quantum harmonic oscillator, $E(0\,K)=\frac{1}{2}\hbar\omega$, plus the phonon contribution (calculated by means of Phonon) defines $E(T)$ = *Eelec* + *ZPE* + *Ephonon*(T). The Helmholtz free energy, $F(T)$, is given by $F(T) = E(T) - TS(T)$, in which $S(T)$ = *Sphonon*(T) is the vibrational entropy at the absolute temperature T. The Helmholtz free energy was assumed to be equal to the Gibbs free energy, since the PV term (in which P is the pressure and V is the volume) can be neglected for solids under the conditions mentioned before.

4. Results and discussion

4.1. Reaction calorimetric method

The room-temperature water solution calorimeter shown in our earlier work [30] was used for the determination of the enthalpy of formation of the $B_{78}Li_{22}$ alloy. The experiments were conducted in a glass crucible. During the dissolution of the $B_{78}Li_{22}$ alloy, the medium (water) was mixed with a stirrer and the values of the thermoelectric power were registered. The determination of the calibration constant was performed with the use of four inorganic compounds: lithium and sodium hydroxides, as well as ice and potassium permanganate. Their heats of solution in water were taken from the Handbook of Chemistry and Physics [39]. The obtained results of the calibration constants together with the values of the reaction heat of lithium (-205.3 kJ/mole) with water were taken from [30]. The samples of the $B_{78}Li_{22}$ alloy were weighed in the glove-box and quickly brought into the calorimeter in a small tightly closed bottle to protect them against the reaction with the air components (H_2O, N_2). Immediately before the measurement, the bottle was opened and the sample was introduced into the water. The values of heat effects and the enthalpy of formation are shown in Table 1 together with the average values and the standard deviation. The calculations were conducted with the assumption of two standard states of boron: amorphous and crystalline, and the results are shown in Table 1. The value of the transition heat of crystalline boron into amorphous boron, at room temperature, was taken from [40]. All the calorimetric data of the enthalpy of formation of the intermetallic compounds from the B-Li system are presented in Fig. 2 and Table 2.

TABLE 2
Standard enthalpy of formation of B-Li intermetallic compounds obtained by the calorimetric reaction method

Phase	Enthalpy of formation Δ_fH [kJ/mol at.]	References
$B_{48}Li_{52}$	-30.3 ±2.2	[31]
B_3Li	-40.8±1.8	[30]
$B_{78}Li_{22}$	-39.0±0.8	This study
$B_{14}Li_3$	-30.1±1.6	[30]
$B_{13}Li$	-10.6±0.1	[30]

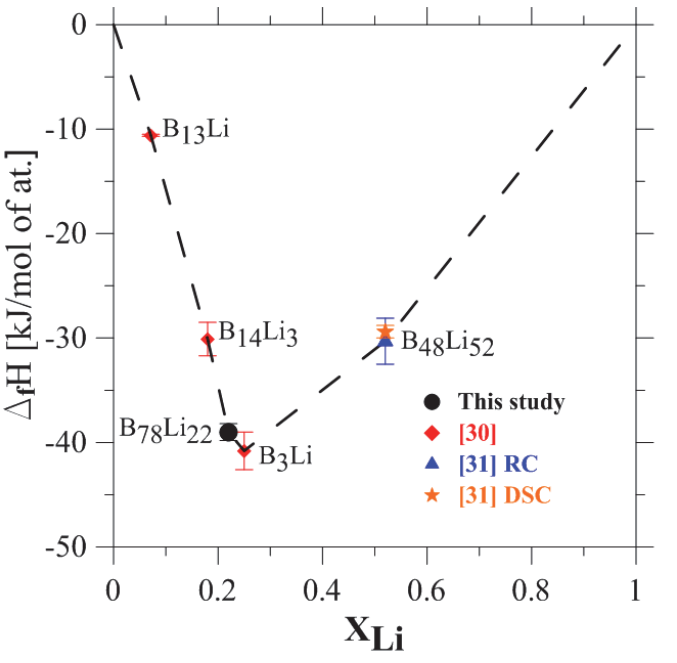

Fig. 2. Standard enthalpy of formation of B-Li intermetallic compounds. RC-reaction calorimetry, DSC- direct synthesis calorimetry

TABLE 1

Heat effects and enthalpy of formation of the $B_{78}Li_{22}$ alloy at 25°C (298 K) obtained by the water reaction calorimetric method

Alloy	T [K]	No of sample	Heat effect ΔH^{ef} [kJ/mol at.]	Enthalpy of formation Δ_{fH} [kJ/mol at.]	Heat effect ΔH^{ef} [kJ/mol at.]	Enthalpy of formation Δ_{fH} [kJ/mol at.]
			Amorphous boron		Crystalline boron	
$B_{78}Li_{22}$	298	1	-2.9	-42.2	-5.9	-39.3
		2	-3.1	-42.1	-6.0	-39.1
		3	-2.8	-42.3	-5.8	-39.4
		4	-4.5	-40.6	-7.5	-37.7
		5	-2.5	-42.7	-5.4	-39.7
		Average value	-3.2	-42.0	-6.1	-39.0
		Standard error	0.7	0.7	0.7	0.7

4.2. DTA measurements

The DTA experiments were performed by means of the Q-1500 derivatograph equipment (Paulik-Paulik-Erdey system) for 14 alloys of the concentrations ranging from 40 to - 100 at% Li. The results of the transition temperatures are shown in Table 3.

TABLE 3

Differential Thermal Analysis data for the B-Li alloys

No of alloy	Li at. %	Transition temperatures °C	
		Heating	Cooling
1	40	809	846
		856	800
2	44	872	842
3	48	817	820
4	52	814	860
		937	803
			786
5	60	798	820
		850	791
6	70	810	834
		844	790
			750
7	74	682	839
		801	815
		833	768
8	77	780	836
		825	810
		841	767
9	80	180	825
		794	779
		836	170
10	85	180	816
		803	789
		835	170
11	90	660	751
			170
12	95	810	802
		834	793
13	98	180	804
		782	796
14	100	181	

4.3. First Principles and Phonon

The experimental data for the enthalpy of formation at 298 K are shown together with the calculated data in Figure 3. The calculated results for X(Li) < 0.17 are in good agreement with the experimental ones. However, the experimental data of the compounds with the Li composition for X(Li) > 0.17 seem to be much more stable than the correspondent calculated ones, although the shape of the curves is very similar. The latter discrepancies are probably associated with the lack of precise calculations of the stability caused by the presence of lithium.

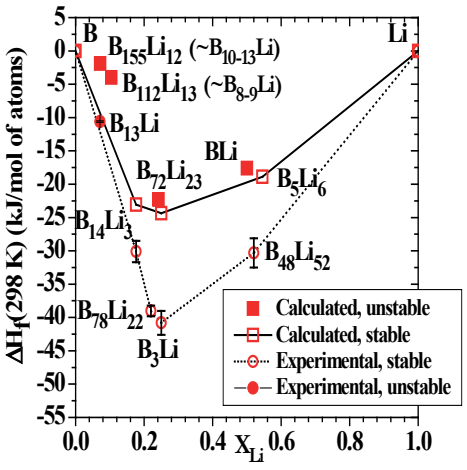

Fig. 3. Calculated and experimental standard enthalpy of formation of B-Li intermetallic compounds

The electronic energy of formation, which corresponds to VASP's energy of formation, is shown in Figure 4. The results presented in Fig. 4 show the same stable compounds as in Fig. 3 and in Fig. 5; meaning that, up to room temperature, only three compounds: $B_{14}Li_3$, B_3Li and B_5Li_6, are stable. This conclusion is, however, not in agreement with the XRD data in Fig. 1, which shows the presence of a phase with $0.176 < X(Li) < 0.220$, for example B_4Li. We studied different B_4Li phases with different crystal structures with up to 300 atoms per unit cell, $B_{42}Li_{11}$, $B_{24}Li_7$, as presented in Fig. 4 and the results show that these phases are far from the stability convex hull. These phases are not expected to be stable at high temperature. Therefore, this study is most likely incomplete, although Herman et al. [29] also show that LiB_4 only becomes stable at 80 GPa. The structure which stabilizes with pressure belongs to the I 4/mmm space group with two formula units per unit cell, like $BaAl_4$ (see 2. In Fig. 4), but its XRD diffraction pattern does not match the one in Fig. 1. Specifically, this pattern does not justify the XRD Bragg peaks occurring at 29º (2θ) and 31º (2θ) (in Fig. 1) and its most intense peak is observed at 49.95º (2θ).

The electronic energy of formation (VASP's energy of formation) presented in Fig. 4 is of the same order of magnitude as the results in [29], indicating that the discrepancy from the experimental results shown in Fig. 3 is of a systematic nature. Contrary to what was presented in [29], at 1 atm., B_3Li is more stable than $B_{14}Li_3$, which is totally in agreement with the experimental results shown in Figure 3. Contrary to [1-2], we could not find a stable phase in the range of compositions of $B_{6\text{-}7}Li$. The most stable phase we found near this composition is $B_{8\text{-}9}Li$. We also reached the conclusion that, at 0 K, B_5Li_6 is more stable than BLi and no homogeneity range is clearly observed in the vicinity of $X(Li) = 0.5$. Likewise, we observed the same huge deviation from the results of [14] with respect to B_4Li_5 (see 9. in Fig. 4), confirming the misassignment hypothesis proposed in [29].

The $B_{155}Li_{12}$ ($\sim B_{10\text{-}13}Li$) compound is not stable at 298 K, according to our calculations presented in Figure 5, although its Gibbs energy of formation stands very close to the convex hull, indicating a non-zero probability of stability for this compound. Likewise, the experimental enthalpy of formation for $B_{13}Li$ at 298 K seems to indicate that, in fact, this compound is not stable at room temperature.

The intermediate compounds' Gibbs free energies calculated at 550 K (277 ºC) are presented in Figure 6. We still find a similar set of stable compounds; nonetheless, $B_{155}Li_{12}$ ($\sim B_{10\text{-}13}Li$) is very near the stable convex hull, indicating that the compound might be stable at this temperature. Moreover, it is also possible that $B_{112}Li_{13}$ ($\sim B_{8\text{-}9}Li$) is stable at this temperature, although its stability is less likely than that of $B_{155}Li_{12}$ ($\sim B_{10\text{-}13}Li$).

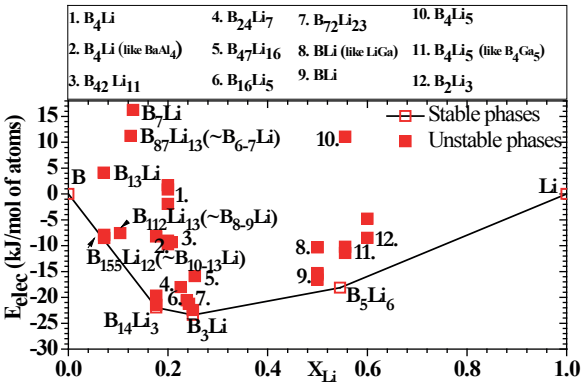

Fig. 4. Electronic energy of formation (VASP's energy of formation) for stable and unstable phases of B-Li intermetallic compounds

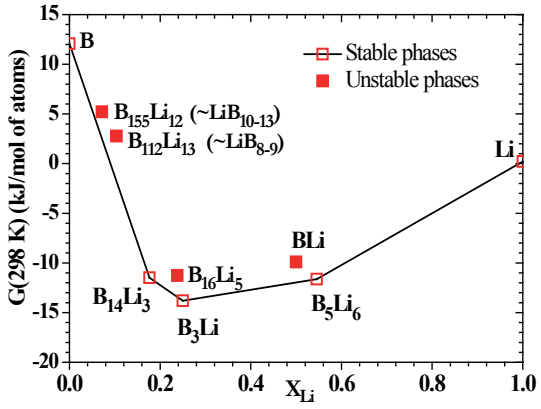

Fig. 5. Gibbs free energy of B-Li intermetallic compounds at 298 K

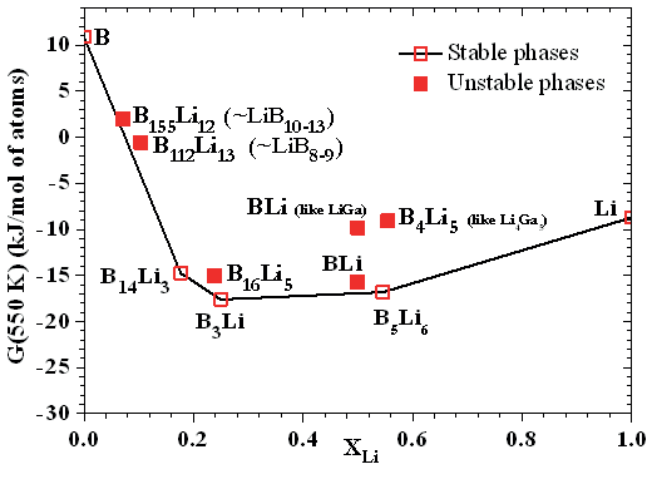

Fig. 6. Calculated Gibbs free energy of B-Li intermetallic compounds at 550 K

At 850 K (577 °C), we finally start to see a homogeneity range from BLi to B_5Li_6. From 550 K to 850 K, $B_{112}Li_{13}$ (~$B_{7-8}Li$) approaches the stable convex hull, contrary to $B_{155}Li_{12}$ (~$B_{10-13}Li$), which gets further apart, although it is still closer to the convex hull than $B_{112}Li_{13}$.

Up till now, we have observed that, at 1050 K (777 °C), the homogeneity range seems to cease to exist and, contrary to what happened at lower temperatures, BLi is the most stable compound. $B_{112}Li_{13}$ (~$B_{8-9}Li$) is even closer to the convex hull, indicating that, probably at probably at higher temperatures, that compound can be stable. $B_{155}Li_{12}$ (~$B_{10-13}Li$) is further away from the stable convex hull.

At the studied temperatures, we could not find a compound with $0.176 < X(Li) < 0.220$ which was stable or presented an XRD pattern that could justify the non-indexed peaks in the XRD of Fig. 1, as highlighted previously.

Observing the phase diagram in Fig. 9, we are able to enumerate the differences between the phase diagram and the first principles calculations:

We could not find a phase with the $B_{6-7}Li$ stoichiometry whose electronic energy of formation (VASP's energy of formation) falls near the stable convex hull. We found a phase with $B_{8-9}Li$ under these conditions;

We could not observe the range of homogeneity around $X(Li) = 0.5$, in the range of temperatures, $T < 850$ K (577 °C);

The range of homogeneity seems to exist around $0.500 \leq X(Li) \leq 0.545$ and between $850\ K < T < 1050$ K;

It is unlikely that $B_{112}Li_{13}$ (~$B_{8-9}Li$) is stable at $T < 1050$ K (777 °C);

It is possible that $B_{155}Li_{12}$ (~$B_{10-13}Li$) is stable at $T \approx 277$ °C, indicating that the compound is more likely to be stable at lower temperatures than $B_{112}Li_{13}$ (~$B_{8-9}Li$).

Similarly to the phase diagram of Fig. 9, $B_{14}Li_3$ and B_3Li are stable compounds in the entire range of temperatures.

The DTA data seems to be in agreement with the calculated features in the homogeneity range of $0.500 \leq X(Li) \leq 0.545$. The eutectic at 453 K can be detected in the samples with $X(Li) \leq 0.545$ [27], indicating that the homogeneity range at this temperature is not as wide as that in the phase diagram's model.

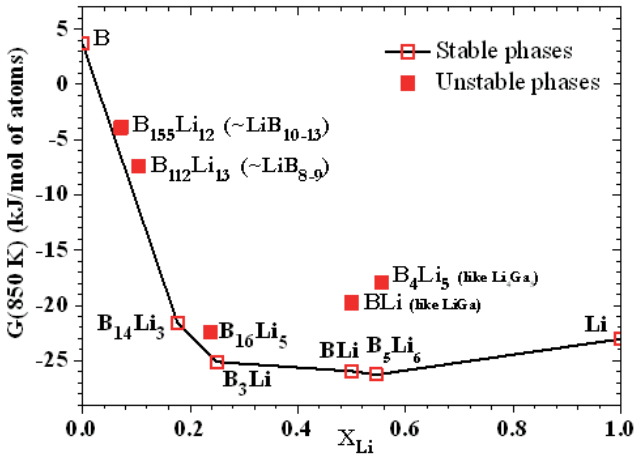

Fig. 7. Calculated Gibbs free energy of B-Li intermetallic compounds at 850 K

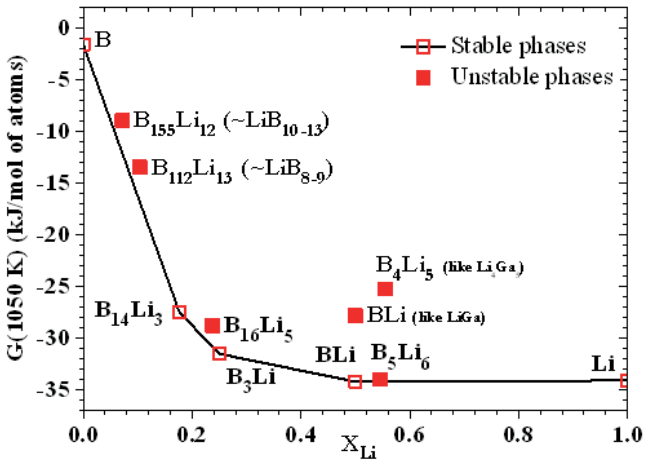

Fig. 8. Calculated Gibbs free energy of B-Li intermetallic compounds at 1050 K

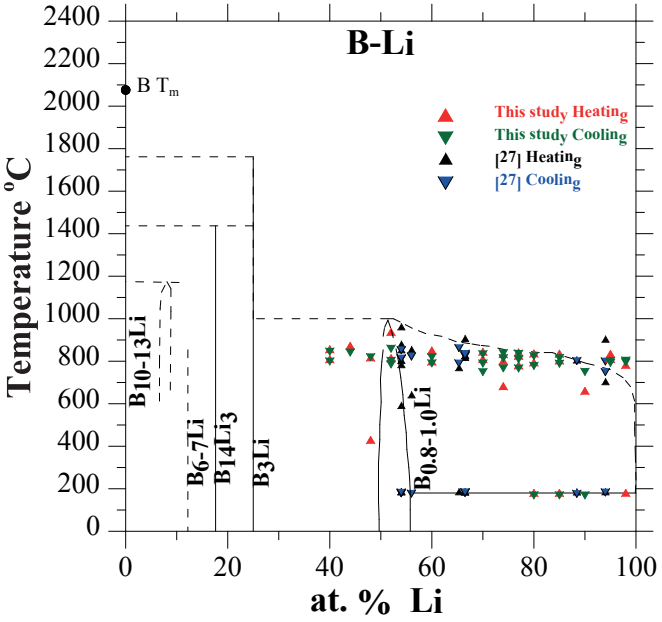

Fig. 9. Phase diagram of B-Li system [26] with data from [27] and our own DTA data

All the experimental results of the standard enthalpy of formation of the intermetallic compounds of the B-Li system obtained from the calorimetric measurements compared with the first principles study are shown in Table 4.

TABLE 4
Standard enthalpy of formation of B-Li intermetallic compound. Experiment vs. first principles study

Phases	$\Delta_f H$ [kJ/mol at.]	
	Experimental	First Principles
B_5Li_6		-18.9
$B_{48}Li_{52}$	-30.3	
B_3Li	-40.8	-24.4
$B_{78}Li_{22}$	-39.0	
$B_{14}Li_3$	-30.1	-23.1
$B_{112}Li_{13}$		-4.0
$B_{155}Li_{12}$		-1.9
$B_{13}Li$	-10.6	

5. Summary

In the present study, we have presented the enthalpy of formation of the $B_{78}Li_{22}$ alloy and its XRD. The alloy is formed by more than one phase. We have concluded that one of the possible phases being part of the $B_{78}Li_{22}$ alloy is B_3Li. The second phase is unknown and we supposed that it could be that suggested by [5], that is B_4Li. With the first principles calculations, we could not find any stable phases in the composition range $0.176 < X(Li) < 0.220$. In this work, we present also the DTA results, as well as the first principles and phonon calculations, which help clarify the previous studies, and also, the phase diagram of the B-Li system. The observed differences between the calculated enthalpies of formation and the calorimetrically measured ones are considerable. The most negative enthalpy of formation was found for the B_3Li compound. The latter conclusion was obtained from the analysis of the experiments and the calculations.

Acknowledgements

The authors wish to express their gratitude to the Ministry of Science and High Education of Poland and the European Union for the financial support of the ZAMAT project (POIG.01.01.02-00-015/09-00), which enabled the realization of the presented investigations.

M.H. Braga is grateful to FCT, Portugal, for the PEst-C/EME/UI0285/2013 support.

REFERENCES

[1] L. Andrieux A. Barbetti, Compt. Rend **194**, 1573 (1932).
[2] L.W. Rupp Jr and D.J. Hodges, J. Phys. Chem. Solids, **35,** 617 (1974).
[3] D.R. Secrist, USAEC Rep. KAPL-**2182,** 33 (1962).
[4] D.R. Secrist, J Am Ceram Soc. **50**, 520 **(**1967).
[5] J. Cassanova French Patent No. 1 461-878 (1965), (H. Okamoto, Bull Alloy Phase Diagr. **1910**, 230 (1989).
[6] L.E. DeVries, L.D. Jackson, S.D. James,. J. Electrochem. Soc., **12,** 993 (1979).
[7] S. Dallek, D.W. Ernst, B.F. Larrick, J. Electrochem. Soc., **126**, 866 (1979).
[8] S.D. James, L.E. DeVries, J. Electrochem. Soc., **123**, 321 (1976).
[9] F.E. Wang, M.A. Mitchell, R.A. Sutula, J.R. Holden, J Less-Common Met **61**, 237 (1978).
[10] V.P. Sorokin, P.I. Gavritov, E.V. Levakov, Zh. Neorg. Khim., **22**, 595 (1977) (in Russian); TR: Russ. J. Inorg. Chem., **22**, 329 (1977).
[11] M.A. Mitchell, R.A. Sutula, J. Less-Common. Met., **57**, 161 (1978).
[12] G. Mair, H.G. Von Schnering, M. Wörle, R. Nesper, Z. Anorg. Allg. Chemie., **625**, 1207 (1999).
[13] G. Mair, R. Nesper, H.G. Von Schnering, J. Solid State Chem., **75**, 30 (1988):.
[14] F.E Wang, M.A. Mitchell, R.A. Sutula, J.R. Holden. J. Less-Common. Met., **61(2)**, 237 (1978).
[15] M. Kobayashi, I. Higashi, H. Matsuda, K. Kimura, J .Alloys Compd., **221**, 20 (1995).
[16] F.E. Wang,. Metall. Trans. A ,**10**, 343 (1979).
[17] P. Sanchez, C. Belin, Compt. Rend. Acad. Sci. Paris Ser. II, **307**, 2027 (1988).
[18] [18]P. Sanchez, C. Belin G. Crepy, A. De Guibert, J. Mater. Sci., 27, 240 (1992).
[19] D. Ernst, J. Electrochem. Soc., **129**, 1513 (1982).
[20] A. Meden, J. Mavri, M. Bele, S. Pejovnik, J. Phys. Chem., **99**, 4252 (1995).
[21] S. Zhang, W. Duan, Z. Liu, Z. Li, X. Qu, Z. Youse. Jinshu Xuebao, **9**, 7 (1999), as reported in Chem. Abstr. 134, 299178w (2000).
[22] Z. Liu, Z. Li, W. Duan, X. Qu, B. Huang. J. Mater. Sci. Technol., **16**, 581 (2000).
[23] T.I. Serebryakova, V.I. Lyashenko, V.D. Levandovskii. Poroshk. Metall., **1-2**, 54. (1994).
[24] [Z.J. Liu, B.Y. Huang, Z.Y. Li. Acta Metal. Sinica., **17**, 667. (2004).
[25] H. Okamoto, Bull. Alloy Phase Diagr., **10**, 230 (1989).
[26] H.B. Borgstedt, C. Gumiński, J. Phase Equilib., **24**, 572 (2003).
[27] T. Marcac, P. Bukovec, N. Bukovec, Thermochim. Acta, **133**, 305 (1988).
[28] S. Aydin, J. Alloys Compd., **569**, 118 (2013).
[29] A. Hermann, A. Mc Sorley, N. W. Ashcroft, R. Hoffmann, J. Am. Chem. Soc., **134**, 18606 (2012).
[30] W. Gąsior, A. Dębski, R. Major, Ł. Major, A. Góral, Intermetallics, **24**, 120 (2012).
[31] W. Gąsior, A. Dębski, R. Major. Arch. Metall. Mater., **59**, 297 (2014).
[32] Powder Diffraction File (ICDD), PDF-4+.
[33] P. Hohenberg, W. Kohn, Phys. Rev. B, **136**, 864 (1964).
[34] J.P. Perdew Y. Wang, Phys. Rev. B, **45**, 13244 (1992).
[35] P. E. Blochl, Phys. Rev. B, **50**, 17953 (1994).
[36] J.P. Perdew, K. Burke, M. Ernzehof, Phys. Rev. Lett., 77, 3865 (1996).
[37] G. Kresse, J. Furthmuller, Phys. Rev. B, 54, 11169 (1996).
[38] K Parlinski, Z.Q. Li, Y. Kawazoe, Phys. Rev. Lett., 78, 4063 (1997).
[39] R.C. Weast, M.J. Astle, WH. Beyer, CRC Handbook of Chemistry and Physics, 66th Edition 1985-1986.
[40] I. Barin, O. Knacke Thermochemical properties of inorganic substances, Springer-Verlag, Berlin, Heidelberg, New York, Verlag Stahleisen m.b.H. Düsseldorf, 1975.

Received: 20 February 2015.